JOURNAL OF GUIDANCE, CONTROL, AND DYNAMICS
Vol. 18, No. 5, September–October 1995

Modeling Issues Related to Retrieval of Flexible Tethered Satellite Systems

Euisok Kim* and Srinivas R. Vadali†
Texas A&M University, College Station, Texas 77843

The retrieval dynamics of the tethered satellite system is simulated using Galerkin's method with and without the contribution of the lateral vibration to the strain and the bead model approach in which the tether is assumed to be a series of point masses connected to each other by massless springs and revolute joints. Simulation results show that all the methods produce significantly different responses. It is found that Galerkin's method without the lateral strain contribution does not reproduce the longitudinal bobbing motion due to lateral vibrations and does not show attenuation of lateral vibrations as the tether shortens. When the lateral contribution is included, convergence of the response is not achieved and sudden divergence is exhibited during retrieval as the number of modes used in the simulation is increased. The simulations using the bead model show the longitudinal bobbing motion as well as the skip-rope motion during the terminal phases of retrieval. In addition, a simple method for obtaining nonrecursive order-N computation for the bead model simulation is presented.

Nomenclature

$\boldsymbol{F}_i$ = known external force vector acting on m_i
$\boldsymbol{R}_0$ = vector from center of Earth to point O
$\boldsymbol{r}_j$ = vector from m_{j+1} to m_j
$\boldsymbol{T}_i$ = tension force vector on m_i due to ith link

Introduction

THE study of the dynamics and control of tethered satellite systems (TSS) has become an area of active research in recent years. The first TSS mission was launched in the late summer of 1992. A comprehensive survey of past studies can be found in Ref. 1. Because of the complexity of the TSS dynamics, various simplifying assumptions are usually made during the derivation of the mathematical models. A table showing the different models used in past studies can be found in Ref. 2. It is noted that there are not many studies in which both three-dimensional vibrations and three-dimensional librations are considered together.

The complexity of the dynamic model is mainly due to the nonlinearity of the equations themselves and the coupling between the three-dimensional vibrations and librations. In a more recent work in which three-dimensional vibrations of the tether are considered, Misra et al.[3] take into account the effect of geometric nonlinearity, or the change in tension due to the transverse curvature of the vibrating tether. In Ref. 3, Galerkin's method is used, and the resulting discretized equations of motion (EOM) are simplified by neglecting the in-plane and out-of-plane librational motion and by assuming only two mode shapes for the vibrations in the lateral directions and one in the longitudinal direction. It was found that inclusion of geometric nonlinearity has a stiffening effect on lateral vibrations. The complete hybrid and discretized forms of the EOM with geometric nonlinearity included can be found in Ref. 4. It should be noted that several terms are neglected by assuming small displacements. Liangdong and Bainum[5] also present the EOM for the TSS discretized by Galerkin's method. However, geometric nonlinearity is not included, and the steady-state value of the tension is used in the equations for the lateral vibrations instead of the actual tension.

Another way to model tethers is to view them as massless springs and point masses (i.e., beads) connected in series. As the number of beads is increased, the system will more closely approximate the continuous tether. One advantage of using the bead model is that the effect of geometric nonlinearity is inherent. A disadvantage is that computational cost can become prohibitive as the number of beads is increased. The deployment/retrieval of the tether modeled in this manner can be simulated, in general, by two methods. In the first method, the mass of each bead and undeformed length between beads are made constant. Deployment/retrieval is simulated by varying the length of the link connected to the shuttle and adding/subtracting a bead from the model at discrete intervals. In the second method, the number of beads is set constant and the mass of the beads and the lengths between the beads are varied uniformly to correspond to the mass and length of the deployed portion of the tether. The commercial software GTOSS[6] incorporates the latter method. The first method is used by Banerjee[7] to simulate both the extrusion of beams and deployment of tethers in which elastic extension between beads is not accounted for. In the present study, the first method, with elastic springs as links, is incorporated.

Many control laws have been proposed to date for the retrieval of TSS.[2–5,8–19] Most are based on a simplified tether model in which the tether is assumed to be either massless and inextensible or to have finite mass but be inextensible and straight. Many of the earlier tension control laws are based on the control law of Rupp.[8] Control laws that are Lyapunov stable can be found in Refs. 12–16. In addition, control laws incorporating feedback of modal coordinates have been proposed in several studies in order to more effectively suppress vibrations.[2–5] He and Powell,[20] using the Euler–Hill equation and linear elasticity, showed that for a tether of constant length, the skip-rope mode is a relatively stable long-term motion and, periodically, the motion alternates between pure rotation and planar lateral motion. This period is of the order of 5 orbits for a 20-km tether and 22 orbits for a 2-km tether of the TSS-1 type.

In this study, the hybrid set of EOM is derived and simulated using Galerkin's method. The bead model is also developed and a nonrecursive order-N method is introduced for efficient computation. Simulation studies of the retrieval process for the TSS and a simplified example will show the following:

1) The Galerkin method without including geometric nonlinearity does not give an accurate representation of the vibrations.

2) When the Galerkin method is used with geometric nonlinearity, a sudden divergence of the response is experienced for certain conditions and number of modes.

3) The bead model simulations exhibit good convergence and appear to capture most of the physics of the problem.

In addition, bead model simulations show that during the terminal phases of retrieval, the tether falls into an almost perfect skip-rope motion. This appears to be true regardless of initial conditions as long as out-of-plane motion is excited.

Received Dec. 16, 1992; revision received Feb. 6, 1995; accepted for publication Feb. 6, 1995.

*Graduate Student, Department of Aerospace Engineering. Student Member AIAA.

†Professor, Department of Aerospace Engineering. Associate Fellow AIAA.

Derivation of the Hybrid Equation of Motion

The following basic assumptions are made for the TSS:

1) The mass of the spacecraft is much larger than the mass of the subsatellite and tether so that the center of mass of the system coincides with the center of mass of the spacecraft at all times.

2) The orbit is circular.

3) The subsatellite is a point mass.

4) There are no disturbances such as atmospheric drag and solar radiation acting on the system.

5) The tether is assumed to be uniform with no torsional or bending rigidity.

The coordinates used are illustrated in Fig. 1. The X, Y, Z frame is the local vertical, local horizontal (LVLH) frame with the Y axis pointing toward the center of Earth. The x, y, z frame is the body fixed frame with the y axis pointing from point O to the subsatellite m. The terms θ and ϕ are the in-plane and out-of-plane libration angles and $u(y, t)$, $v(y, t)$ and $w(y, t)$ are the x, y, and z components of the displacement of a point originally at a distance y from the origin along the y axis. Here, l is the instantaneous undeformed length of the tether and Ω is the orbital rate.

For any element dy on the tether, originally at a distance y from the origin O, the position vector $\boldsymbol{R}$ is given by

$$\boldsymbol{R} = \boldsymbol{R}_0 + \boldsymbol{r} \tag{1}$$

$$\boldsymbol{r} = \begin{Bmatrix} u \\ y+v \\ w \end{Bmatrix} \text{ in } x,\ y,\ z \text{ components}$$

Then, the inertial acceleration $\boldsymbol{a}_I$ is simply $\boldsymbol{a}_I = \mathrm{d}^2\boldsymbol{R}/\mathrm{d}t^2$.

The gravity-gradient force $\boldsymbol{F}_G$ acting on the tether element dy is obtained by

$$\boldsymbol{F}_G = \frac{-\mu\rho\,\mathrm{d}y}{|\boldsymbol{R}_0+\boldsymbol{r}|^3}(\boldsymbol{R}_0+\boldsymbol{r}) \tag{2a}$$

$$\approx -\rho\,\mathrm{d}y\Omega^2\left[\boldsymbol{R}_0+\boldsymbol{r}-\frac{3(\boldsymbol{R}_0\cdot\boldsymbol{r})}{|\boldsymbol{R}_0|}\boldsymbol{R}_0\right] \tag{2b}$$

where ρ is the mass per unit length of the tether and μ is the universal gravitational constant. Here, binomial expansion is performed on the fraction in Eq. (2a) and terms up to first order in $\boldsymbol{r}$ are retained to obtain Eq. (2b). Since the system is assumed to be in circular orbit, the relation $\Omega = \sqrt{\mu/|R_0|^3}$ is used.

Equation (2b) can be written in the form $\boldsymbol{F}_G = -\rho\,\mathrm{d}y\,\boldsymbol{a}_G$ where $\boldsymbol{a}_G$ is the acceleration acting on the element dy due to gravity. After considerable algebra, the body coordinate components of the total acceleration $\boldsymbol{a} \equiv \boldsymbol{a}_I + \boldsymbol{a}_G$ are obtained as

$$\begin{aligned} a_x &= \ddot{u} - (y+v)\ddot{\phi} - w\ddot{\theta}S_\phi - 2(\dot{l}+\dot{v})\dot{\phi} - 2\dot{w}(\Omega+\dot{\theta})S_\phi \\ &\quad - u\left[(\Omega+\dot{\theta})^2 S_\phi^2 + \dot{\phi}^2\right] - (y+v)(\Omega+\dot{\theta})^2 C_\phi S_\phi \\ &\quad + \Omega^2\left[u\left(1-3C_\theta^2 S_\phi^2\right) - 3(y+v)C_\theta^2 C_\phi S_\phi + 3wC_\theta S_\theta S_\phi\right] \end{aligned} \tag{3a}$$

$$\begin{aligned} a_y &= \ddot{l} + \ddot{v} + u\ddot{\phi} - w\ddot{\theta}C_\phi + 2\dot{u}\dot{\phi} - 2\dot{w}(\Omega+\dot{\theta})C_\phi \\ &\quad - (y+v)\left[(\Omega+\dot{\theta})^2 C_\phi^2 + \dot{\phi}^2\right] - u(\Omega+\dot{\theta})^2 C_\phi S_\phi + \Omega^2 \\ &\quad \times\left[-3uC_\theta^2 C_\phi S_\phi + (y+v)\left(1-3C_\theta^2 C_\phi^2\right) + 3wC_\theta S_\theta C_\phi\right] \end{aligned} \tag{3b}$$

$$\begin{aligned} a_z &= \ddot{w} + [uS_\phi + (y+v)C_\phi]\ddot{\theta} + 2\dot{u}(\Omega+\dot{\theta})S_\phi \\ &\quad + 2(\dot{l}+\dot{v})(\Omega+\dot{\theta})C_\phi + 2u(\Omega+\dot{\theta})\dot{\phi}C_\phi - w(\Omega+\dot{\theta})^2 \\ &\quad - 2(y+v)(\Omega+\dot{\theta})\dot{\phi}S_\phi + \Omega^2\left[3uC_\theta S_\theta S_\phi\right. \\ &\quad \left. + 3(y+v)C_\theta S_\theta C_\phi + w\left(1-3S_\theta^2\right)\right] \end{aligned} \tag{3c}$$

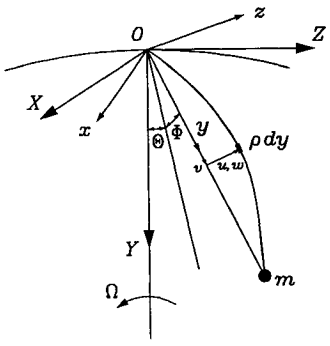

Fig. 1 Continuous model coordinate systems.

As in Refs. 3 and 4, it can be shown that the longitudinal strain is

$$\epsilon = \frac{\mathrm{d}s - \mathrm{d}y}{\mathrm{d}y} \approx \frac{\partial v}{\partial y} + \frac{1}{2}\left[\left(\frac{\partial u}{\partial y}\right)^2 + \left(\frac{\partial w}{\partial y}\right)^2\right] \tag{4}$$

where ds and dy are, respectively, the stretched and unstretched lengths of an element of the tether. The second term on the right-hand side of Eq. (4) is the term that accounts for the geometric nonlinearity. Depending on one's point of view, it can be interpreted as either a foreshortening effect or a tension augmentation effect due to lateral displacements or both. Assuming small angles, tension force components acting on the element dy are found to be

$$\boldsymbol{T} = EA\begin{Bmatrix} \dfrac{\partial u}{\partial y}\left\{\dfrac{\partial v}{\partial y} + \dfrac{1}{2}\left[\left(\dfrac{\partial u}{\partial y}\right)^2 + \left(\dfrac{\partial w}{\partial y}\right)^2\right]\right\} \\ \dfrac{\partial v}{\partial y} + \dfrac{1}{2}\left[\left(\dfrac{\partial u}{\partial y}\right)^2 + \left(\dfrac{\partial w}{\partial y}\right)^2\right] \\ \dfrac{\partial w}{\partial y}\left\{\dfrac{\partial v}{\partial y} + \dfrac{1}{2}\left[\left(\dfrac{\partial u}{\partial y}\right)^2 + \left(\dfrac{\partial w}{\partial y}\right)^2\right]\right\} \end{Bmatrix} \tag{5}$$

The force balance equation for the element dy yields the EOM of the tether,

$$\rho\,\mathrm{d}y\,\boldsymbol{a} = \frac{\partial \boldsymbol{T}}{\partial y}\,\mathrm{d}y \tag{6}$$

The moment balance equation for the complete system about the origin is

$$\boldsymbol{M} = \int_0^l \rho\boldsymbol{r}\times\boldsymbol{a}\,\mathrm{d}y + m\boldsymbol{r}_l\times\boldsymbol{a}_l \tag{7}$$

where $\boldsymbol{M}$ is the moment due to external elements such as control thrusters and subscript l indicates that the value is evaluated at $y = l$. The equations for the in-plane and out-of-plane libration angles θ and ϕ are obtained by taking the x and z components of Eq. (7).

Finally, the equations at the boundaries can be obtained by equating the y component of the tension forces to the y component of the inertial and gravitational forces at each end,

$$-T(0, t) = \int_0^l \rho\,\boldsymbol{a}_y\,\mathrm{d}y + m[\boldsymbol{a}_y]_l \tag{8a}$$

$$-T(l, t) = m[\boldsymbol{a}_y]_l \tag{8b}$$

and by the geometric relations

$$u(0, t) = w(0, t) = u(l, t) = w(l, t) = 0 \tag{8c}$$

Equations (6–8) are discretized by expanding the vibrational displacements u, v, and w as follows:

$$u(y,t) = \sum_{i=1}^{n} \phi_i(y,l) A_i(t) \tag{9a}$$

$$w(y,t) = \sum_{i=1}^{n} \phi_i(y,l) C_i(t) \tag{9b}$$

$$v(y,t) = v_s(y,l) + \sum_{i=1}^{n} \psi_i(y,l) B_i(t) \tag{9c}$$

where

$$\phi_i(y,l) = \sin\left(\frac{i\pi y}{l}\right) \qquad \psi_i(y,l) = \left(\frac{y}{l}\right)^i$$

Here, $v_s(y,l)$ is the static deformation of the tether when the tether is statically aligned with the local vertical axis and is obtained explicitly in Ref. 19 as

$$v_s(y,l) = B(l)\sin(k_1 y) - y \tag{10}$$

where

$$B(l) = \frac{1}{k_1\cos(k_1 l) - k_2\sin(k_1 l)}$$

$$k_1 = \Omega\sqrt{\frac{3\rho t}{EA}} \qquad k_2 = \frac{3m\Omega^2}{EA}$$

The conversion of Eqs. (6–8) into the weak form is done in the usual manner as outlined clearly in Ref. 3. It should be noted at this point that the discretization procedure given above is not the Galerkin method in the classical sense since ψ_i do not in general satisfy all the boundary conditions and ϕ_i and ψ_i are implicit functions of time due to the time dependence of l. Although this method of discretizing the equations of deployable continuous systems is rather commonly used, the validity of using such time-dependent shape functions has not yet been rigorously proved.[7]

The amount of effort required to discretize all the equations is quite enormous, mainly due to the large number of different integrals generated as a result of the time dependence of the shape functions. The symbolic manipulator program MACSYMA was used extensively to evaluate many of the integrals so that up to seven modes in both the lateral and longitudinal degrees of freedom can be simulated.

Bead Model

The coordinate system used for the bead model is illustrated in Fig. 2. The tether is assumed to be a series of point masses connected by N massless springs of constant undeformed lengths. The extension of the ith spring with spring constant k_i is v_i. The revolute joints between the masses and springs are assumed to be frictionless. For the Nth link, it is assumed that the segment from the shuttle to the anchor point o (length b) is inextensible, and point o is connected to the Nth mass by the Nth spring. The mass of the ith bead for $i = 2, \ldots, N-1$ is calculated as $m_i = (1/2)\rho(l_{i-1} + l_i)$. The mass of the first bead, m_1, equals $m + (1/2)\rho l_1$. The mass of the Nth bead is $\rho(l_{(N-1)}/2 + l_N + b)$. The lengths of the links are chosen such that $\sum_{i=1}^{N-1} l_i + l_N + b = l$, the total undeformed of the tether. The spring constants are obtained by equating the deformation of each bead in the bead model to the deformation of the points on the continuous tether corresponding to the bead when both models are subjected to an axial force of equal magnitude applied to one end of the tether. Thus,

$$k_i = \begin{cases} EA/l_i & \text{if} \quad i < N \\ EA/(l_N + b) & \text{if} \quad i = N \end{cases} \tag{11}$$

The tether is deployed/retrieved by varying the length b and the number of beads. During retrieval, at the instant when b becomes zero, the Nth mass disappears and a new anchor point is defined. Then N is set to $N-1$. The reverse holds for deployment. This concept of using an anchor point is similar to that in Ref. 7 except that, in this study, the segment b is allowed to rotate freely about point O. It is necessary to define the anchor point in order to avoid numerical singularities that will occur during retrieval as the length of the Nth link tends to zero.

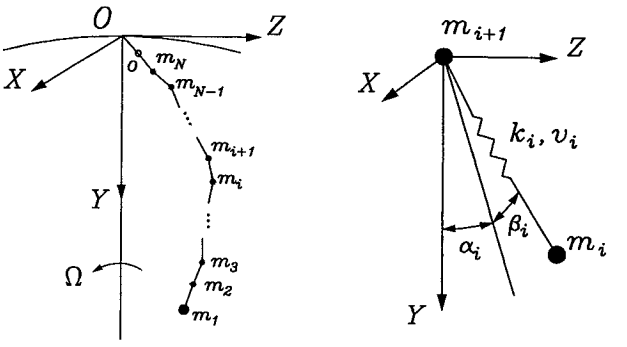

Fig. 2 Bead model coordinate systems.

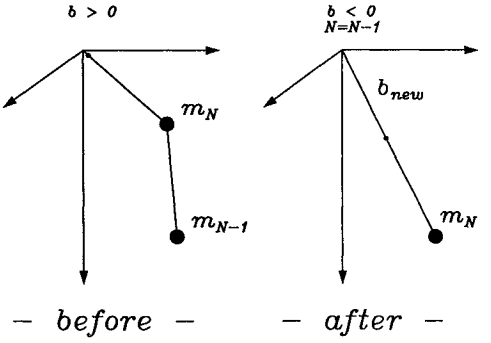

Fig. 3 Discontinuity as Nth bead is retracted.

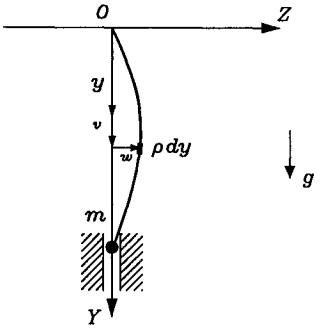

Fig. 4 Simplified system schematics.

Figure 3 illustrates what happens when $b < 0$ and the Nth bead is retracted. The new states (α_N, $\dot{\alpha}_N$, β_N, $\dot{\beta}_N$, v_N, $\dot{v}_N$, and b) for the new Nth bead [previously the $(N-1)$th bead] must be reinitialized so as to enforce continuity in the displacements and velocities of the new Nth mass. Hence there are six continuity conditions that must be satisfied. Since there are seven variables, an additional continuity requirement for the tension of the Nth link can be enforced. The resulting equations for the new initial conditions of variables of the Nth mass and link are

$$\alpha_N = \tan^{-1}\left(\frac{Z_N}{Y_N}\right) \tag{12a}$$

$$\beta_N = \tan^{-1}\left(\frac{-X_N\cos\alpha_N}{Y_N}\right) \tag{12b}$$

$$b = \frac{(l_N^- + b^-)\left[\sqrt{X_N^2 + Y_N^2 + Z_N^2} - l_N\right] - v_N^- l_N}{l_N^- + b^- + v_N^-} \tag{12c}$$

$$v_N = \frac{v_N^-(l_N + b)}{l_N^- + b^-} \tag{12d}$$

$$\dot{\alpha}_N = \frac{\dot{Z}_N\cos\alpha_N - \dot{Y}_N\sin\alpha_N}{(l_N + b + v_N)\cos\beta_N} \tag{12e}$$

$$\dot{\beta}_N = \frac{-(\dot{X}_N \cos\alpha_N + \dot{Y}_N \cos\alpha_N \sin\alpha_N + \dot{Z}_N \sin\alpha_N \sin\beta_N)}{(l_N + b + v_N)} \tag{12f}$$

$$\dot{v}_N = (\dot{Y}_N \cos\alpha_N + \dot{Z}_N \sin\alpha_N)\cos\beta_N - \dot{X}_N \sin\beta_N - \dot{b} \tag{12g}$$

where X_N, Y_N, and Z_N are the displacements in the LVLH frame components of the current Nth mass [previous $(N-1)$th mass] at the instant before a mass is taken away, and v_N^-, l_N^-, and b^- are the longitudinal elastic extension, undeformed segment length, and anchor point distance of the previous Nth link, respectively. Note that Eqs. (12) can be solved sequentially in the order presented.

The EOM can be derived by taking the force equilibrium for the ith bead. This yields

$$m_i \sum_{j=i}^{N} \frac{\mathrm{d}^2 \boldsymbol{r}_j}{\mathrm{d}t^2} = -\boldsymbol{T}_i + \boldsymbol{T}_{i-1} + \boldsymbol{F}_i - m_i \Omega^2 \sum_{j=i}^{N} \boldsymbol{r}_j + \frac{3m_i \Omega^2 \left(\boldsymbol{R}_0 \cdot \sum_{j=i}^{N} \boldsymbol{r}_j\right)\boldsymbol{R}_0}{|\boldsymbol{R}_0|^2} \tag{13}$$

The tension force vector can be obtained by the relation

$$\boldsymbol{T}_i = k_i v_i \hat{\boldsymbol{e}}_{y_i} \tag{14}$$

where $\hat{\boldsymbol{e}}_{y_i}$ is the unit vector along the ith link.

In order to closely match the response of the continuous tether, the number of beads used in the model must be sufficiently high. As the number of beads N increases, computation cost for the simulation becomes a concern. It is well known that, for multibody problems, computational cost can in some cases increase proportional to N^3 or even N^4. Hence, development of algorithms in which computational cost increases proportional to N (order-N algorithms) has been a subject of active research for some time. If, in addition to being order N, the algorithm is nonrecursive, computational time may be reduced even further by the use of parallel processing. In the following, Eq. (13) will be modified in several simple steps in order to develop a nonrecursive order-N algorithm for the bead model.

First, the ith and $(i+1)$th equations of Eq. (13) are divided by m_i and m_{i+1}, respectively. After subtracting the resulting $(i+1)$th equation from the resulting ith equation, one obtains, for $i = 1, 2, \ldots, N$,

$$\frac{\mathrm{d}^2 \boldsymbol{r}_i}{\mathrm{d}t^2} = \frac{\boldsymbol{T}_{i-1}}{m_{i+1}} - \left(\frac{1}{m_i} + \frac{1}{m_{i+1}}\right)\boldsymbol{T}_i + \frac{\boldsymbol{T}_{i+1}}{m_{i+1}} + \frac{\boldsymbol{F}_i}{m_i} - \frac{\boldsymbol{F}_{i+1}}{m_{i+1}} - \Omega^2 \boldsymbol{r}_i + \frac{3\Omega^2 (\boldsymbol{R}_0 \cdot \boldsymbol{r}_i)\boldsymbol{R}_0}{|\boldsymbol{R}_0|^2} \tag{15}$$

where it is understood that $\boldsymbol{T}_0 = \boldsymbol{T}_{N+1} = 0$ and $m_{N+1} = \infty$.

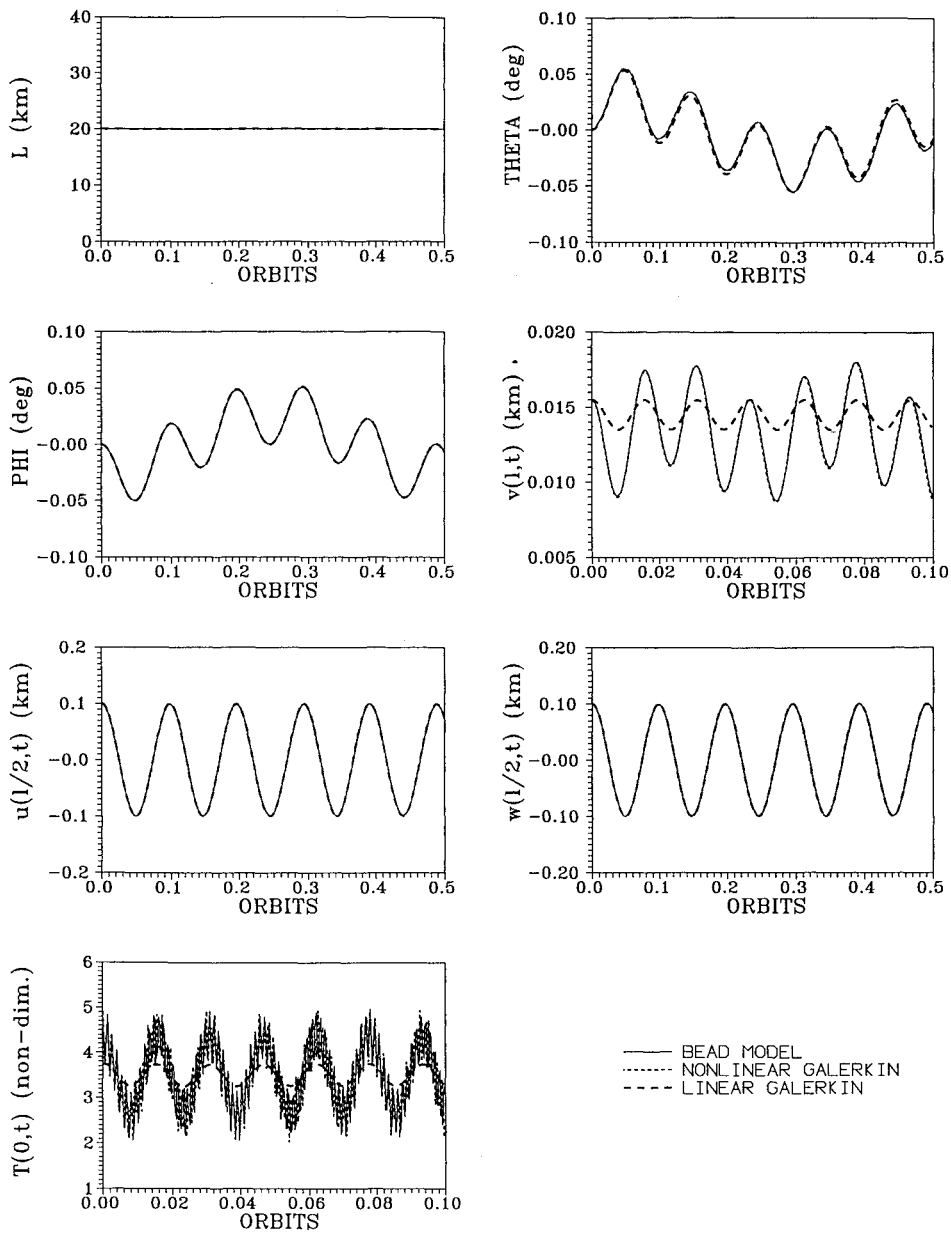

Fig. 5 Constant-length tether simulation results for orbiting system [Galerkin models with (3, 3) modes and bead model with 40 beads].

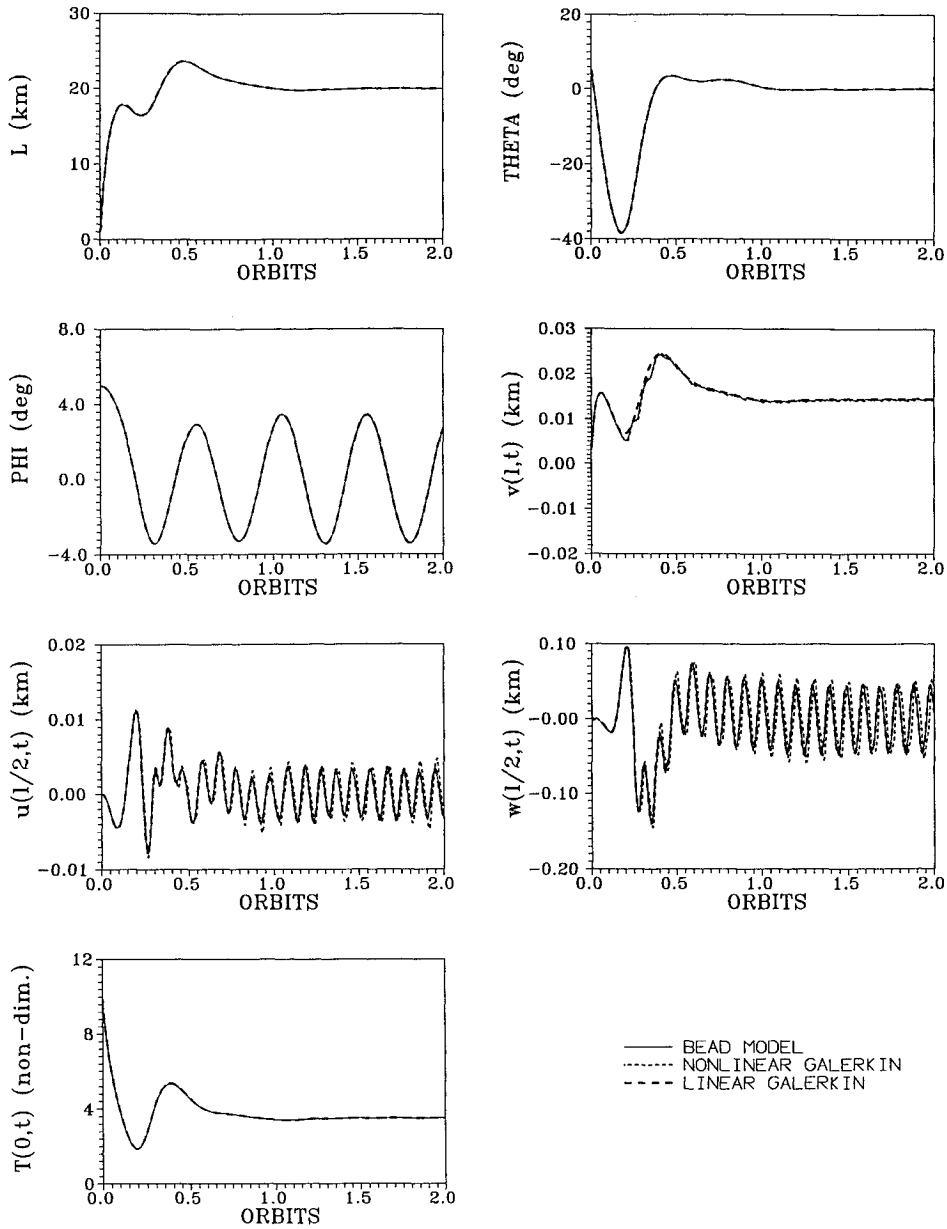

Fig. 6 Deployment simulation results for orbiting system [Galerkin models with (3, 3) modes and bead model with 80 beads].

By expanding the resulting equation in terms of the variables α_i, β_i, and v_i and taking the components of Eq. (15) along any desired frame components, the following form can be obtained:

$$\left[M^i_{jk}\right]\begin{Bmatrix}\ddot{v}_i\\ \ddot{\alpha}_i\\ \ddot{\beta}_i\end{Bmatrix} = \left\{f^i_j\right\} \tag{16}$$

Here, M^i_{jk} and f^i_j are the elements of a 3 × 3 matrix and a 3 × 1 column matrix, respectively, and are explicit functions of the system coordinates, their velocities, and known external forces.

The algorithm for solution is simply the following:

1) Calculate the entries of $[M^i_{jk}]$ and $\{f^i_j\}$.

2) Solve

$$\begin{Bmatrix}\ddot{v}_i\\ \ddot{\alpha}_i\\ \ddot{\beta}_i\end{Bmatrix} = \left[M^i_{jk}\right]^{-1}\left\{f^i_j\right\}$$

3) Repeat steps 1 and 2 for all i.

Obviously, the algorithm is nonrecursive since the acceleration for one bead does not depend on the acceleration of another, and the calculations required by Eqs. (16) are not dependent on any previous calculations. In addition, the algorithm is order N because a fixed number of calculations is required for each bead regardless of how many beads are used.

Results and Discussion

In addition to the complete TSS orbiting Earth in a circular orbit, a simplified example is also simulated to better illustrate the effects of geometric nonlinearity and the characteristics of the different simulation methods. In the simplified example shown in Fig. 4, the shuttle is assumed to be inertially fixed. Only planar motion is considered and the subsatellite is assumed to be constrained to move only in the vertical direction, for the purpose of eliminating the effects of rotational dynamics, while allowing vertical motion due to geometric nonlinearity. The control law used for the simulation is derived in Refs. 14 and 15.

The common parameters for both of the simulations are m = 500 kg, ρ = 8.35 kg/km, and EA = 61,645 N. For the orbiting system, the circular orbit altitude in 297 km. For the simplified example, the gravitational acceleration is defined such that the static tension values for both the orbiting and simplified systems are equivalent at the shuttle/tether attachment points when the tether length is 20 km. Here, l_f for retrieval is 1.0 km. The vibrations are excited by giving initial displacements denoted by Amp = ($Ampx$, $Ampy$, $Ampz$)

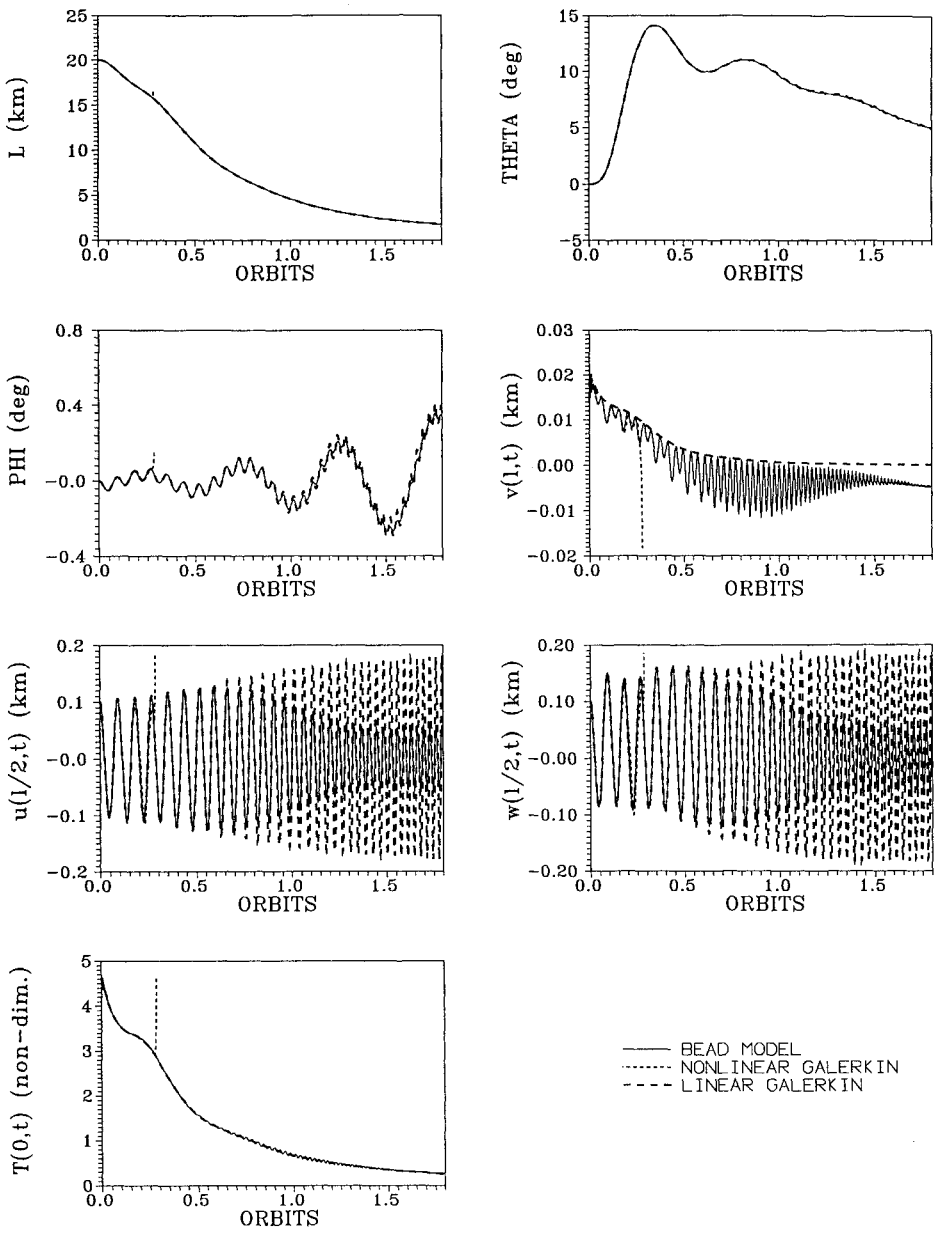

Fig. 7 Retrieval simulation results for orbiting system [Galerkin models with (3, 3) modes and bead model with 80 beads].

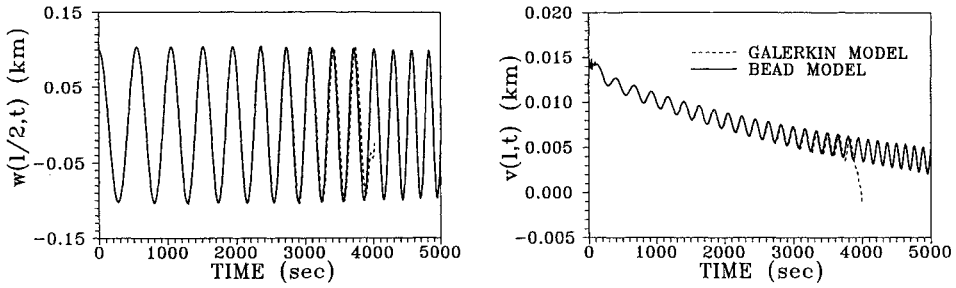

Fig. 8 Retrieval simulation results for simplified system [nonlinear Galerkin model, (3, 3) modes vs bead model, 40 beads].

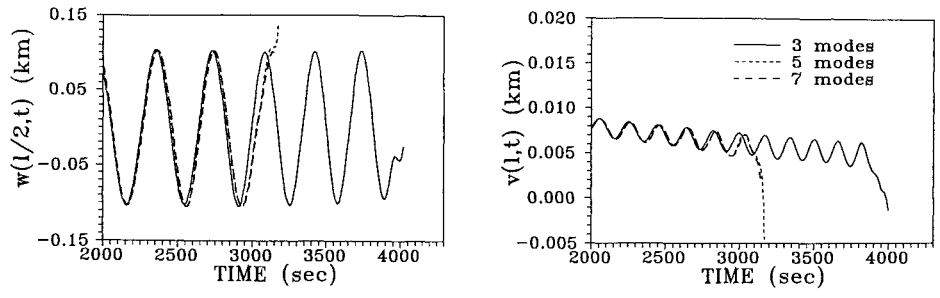

Fig. 9 Effect of increasing number of modes during retrieval.

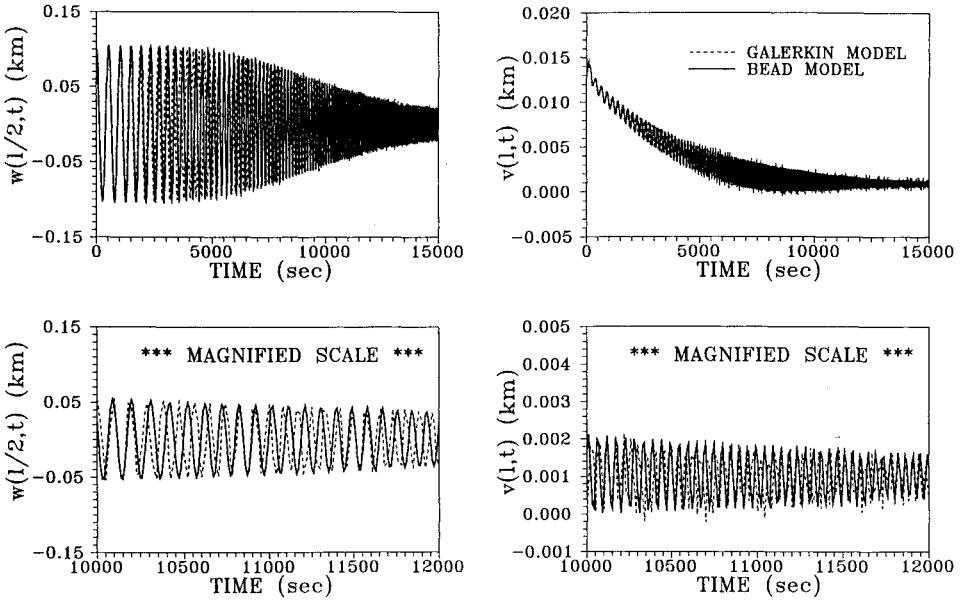

Fig. 10 Retrieval simulation results for simplified system [nonlinear Galerkin model, (2, 1) modes vs bead model, 40 beads].

where $Ampx$, $Ampy$, and $Ampz$ are the first modal coordinate amplitudes for u, v, and w, respectively. The legend Linear Galerkin corresponds to the response of the full nonlinear Galerkin model with geometric nonlinearity neglected, and the legend Nonlinear Galerkin corresponds to the model with geometric nonlinearity included.

First, simulation results of the orbiting TSS are presented. Figure 5 shows the uncontrolled response when the length l is set constant at 20 km and initial vibrational displacements are $Amp = (0.1, 0.001, 0.1)$. Three modes are used for the lateral and longitudinal coordinates. The results for all the models correlate very well with each other except for the longitudinal displacement $v(y, t)$ at $y = l$ and the tension at the shuttle attach point. The linear Galerkin model does not match either $v(l, t)$ or $T(0, t)$ simulations well, whereas the nonlinear Galerkin and bead models match well for the longitudinal response. Note that tension is nondimensionalized with respect to $m\Omega^2 L$, where Ω is the orbital rate and L is the maximum tether length.

Figure 6 shows the response for deployment. Initial in-plane out-of-plane angles are 5.0 deg and initial deployment velocity is 0.7 km/s. It can be seen that during deployment vibrational amplitudes do not grow, and the response for all the models agree very well.

When the system is retrieved with initial displacements $Amp = (0.1, 0, 0.1)$, the simulation results up to approximately 0.3 orbits (Fig. 7) match well between all the models for all the outputs except the longitudinal deformation at $y = l$. The three models show the effectiveness of the tension control law in attenuating the high-frequency longitudinal vibrations in the initial stages of retrieval. This is in accordance with the findings in Ref. 19. However, the bead and nonlinear models show continuing longitudinal oscillations with frequency two times that of the lateral vibrations. This motion is the foreshortening effect due to the geometric nonlinearity and is absent in the longitudinal response of the linear Galerkin model. During the latter part of the retrieval process, it can be seen that even the lateral vibrations of the linear model begin to deviate significantly from the bead model response. The lateral vibrational amplitudes are attenuated in the bead model response as predicted, but this is not true for the linear Galerkin model.

At approximately 0.3 orbits, the nonlinearity Galerkin model response diverges abruptly and the simulation was not able to continue further. This phenomenon occurred at almost the exact point regardless of the integration scheme used. Thus, it does not appear to be attributable to the numerical integration scheme. It is felt that the instability is introduced due to the discretization procedure and manifests itself during retrieval.

The effect of geometric nonlinearity and the shortcomings of Galerkin's method for simulation of the TSS are further shown in the simulation studies of the simplified example. The vibrational response when the nonlinear Galerkin model is used with three lateral and longitudinal modes (Fig. 8) shows that, as in the orbiting TSS simulations, the system diverges suddenly during retrieval although the responses up to the point of divergence correlate very well with those of the bead model. Figure 9 illustrates how the divergence occurs earlier as the number of modes are increased. It appears that after five modes the point of divergence remains nearly stationary. It was found that the nonlinear Galerkin model of the full system in orbit exhibits the same trend.

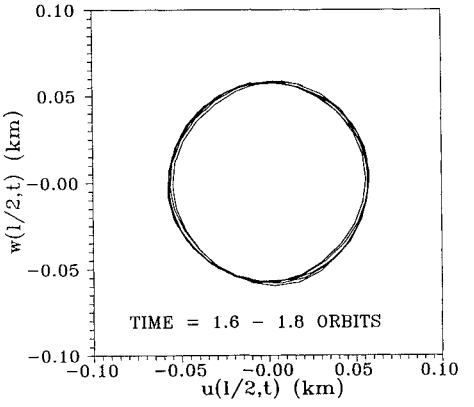

Fig. 11 Skip-rope motion during end of retrieval.

In Fig. 10, the simulation is carried out with two modes used for $w(y, t)$ and one mode used for $v(y, t)$. Although frequencies of oscillations do not match, the vibrational amplitudes of the nonlinear Galerkin model show trends similar to the bead model response. This supports the presumption that the bead model produces responses closest to the actual dynamic system responses. Similar attempts to duplicate amplitude trends for the orbiting TSS were not successful. Although the use of one mode in the lateral vibrational coordinate with the nonlinear Galerkin model allowed the simulation to proceed up to the end of retrieval, amplitude responses did not correlate well with those of the bead model.

An interesting phenomenon can be observed in the bead model response shown in Fig. 7. It is observed that at the end of the simulation the lateral vibrational amplitudes $u(l/2, t)$ and $w(l/2, t)$ level off to the same magnitude. At the same time, the oscillatory motion of the longitudinal displacement $v(l, t)$ dies out and the mean displacement value decreases to below zero. This can be explained by Fig. 11. It is realized that the bead model has fallen into an almost perfectly symmetric skip-rope motion. The

longitudinal displacement is therefore continually negative because of foreshortening due to an almost constant curvature of the tether. A simple calculation shows that the magnitude of the longitudinal displacement observed at the final time coincides with the amount of foreshortening that would exist when the tether shape is assumed to be a sine function. Additional simulations showed the skip-rope motion occurred for all the initial conditions used in which there is initial out-of-plane excitation.

Conclusions

A detailed continuous model of the TSS that includes the effects of tether flexibility and a bead model that allows for longitudinal elongation and lateral deflections are developed. When geometric nonlinearity is included, a sudden divergence occurs during mid-retrieval when a sufficient number of modes is used to discretize the system equations using the Galerkin method. The divergence is not seen during deployment. The exact cause of the divergence is unknown but is suspected to be artificial and a result of applying the Galerkin discretization procedure with time-dependent shape functions to the naturally unstable retrieval dynamics of the TSS. When geometric nonlinearity is excluded, longitudinal vibrational response and lateral vibrational responses during the latter phases are not accurate as the expected bobbing motions due to foreshortening effects and lateral vibrational amplitude attenuation are not exhibited.

The bead model appears to produce the most realistic response. The simulation results match well with the nonlinear Galerkin model up to the point of divergence, and the expected effects of geometric nonlinearity were present. These effects are found to be quite significant. In addition, a nonrecursive order-N method for simulating the bead model that is computationally efficient and has potential parallel computer application is introduced.

Finally, it is observed from additional bead model simulation results that the tether falls into an almost perfect skip-rope motion during the end of retrieval for all the initial conditions for which out-of-plane motion is excited.

Acknowledgment

This research was supported by the Texas Higher Education Coordinating Board under ATP Grant 999903-264.

References

[1]Misra, A. K., and Modi, V. J., "A Survey on the Dynamics and Control of Tethered Satellite Systems," *Tethers in Space, Advances in the Astronautical Sciences*, Vol. 62, American Astronautical Society, San Diego, CA, 1987, pp. 667–719.

[2]Misra, A. K., and Modi, V. J., "Deployment and Retrieval of a Subsatellite Connected by a Tether to the Space Shuttle," *Journal of Guidance, Control, and Dynamics*, Vol. 5, No. 3, 1982, pp. 278–285.

[3]Misra, A. K., Xu, D. M., and Modi, V. J., "On Vibrations of Orbiting Tethers," *Acta Astronautica*, Vol. 13, No. 10, 1986, pp. 587–597.

[4]Xu, D. M., "Dynamics and Control of Shuttle Supported Tethered Satellite Systems," Ph.D. Dissertation, Dept. of Mechanical Engineering, McGill Univ., Montreal, Canada, 1984.

[5]Liangdong, L., and Bainum, P. M., "Effect of Tether Flexibility on the Tethered Shuttle Subsatellite Stability and Control," *Journal of Guidance, Control, and Dynamics*, Vol. 12, No. 6, 1989, pp. 866–873.

[6]Lang, D. D., *GTOSS Manual*, Lang and Associates, Seattle, WA, July 1991.

[7]Banerjee, A. K., "Order-n Formulation of Extrusion of a Beam with Large Bending and Rotation," *Journal of Guidance, Control, and Dynamics*, Vol. 15, No. 1, 1992, pp. 121–127.

[8]Rupp, C. C., "A Tethered Tension Control Law for Tethered Subsatellites Deployed Along the Local Vertical," NASA TMX-64963, Sept. 1975.

[9]Baker, W. P., Dunkin, J. A., Galabott, Z. J., Johnston, K. D., Kissel, R. R., Rheinfurth, M. H., and Giebel, M. P. L., "Tethered Subsatellite Study," NASA TMX-73314, March 1976.

[10]Bainum, P. M., and Kumar, V. K., "Optimal Control of the Tethered Subsatellite System," *Acta Astronautica*, Vol. 7, No. 5, 1980, pp. 1333–1348.

[11]Modi, V. J., Chang-fu, G., Misra, A. K., and Xu, D. M., "On the Control of the Space Shuttle Based Tethered System," *Acta Astronautica*, Vol. 9, No. 6/7, 1982, pp. 437–443.

[12]Fujii, H., and Ishijima, S., "Mission Control for Deployment and Retrieval of a Subsatellite," *Journal of Guidance, Control, and Dynamics*, Vol. 12, No. 2, 1989, pp. 243–247.

[13]Vadali, S. R., "Feedback Tether Deployment and Retrieval," *Journal of Guidance, Control, and Dynamics*, Vol. 14, No. 2, 1991, pp. 469–470.

[14]Vadali, S. R., and Kim, E., "Feedback Control of Tethered Satellites Using Lyapunov Stability Theory," *Journal of Guidance, Control, and Dynamics*, Vol. 14, No. 4, 1991, pp. 729–735.

[15]Kim, E., and Vadali, S. R., "Nonlinear Feedback Deployment and Retrieval of Tethered Satellite Systems," *Journal of Guidance, Control, and Dynamics*, Vol. 15, No. 1, 1992, pp. 28–34.

[16]Monshi, N., Misra, A., and Modi, V. J., "A Parametric Study on the Reel Rate Control of Retrieval Dynamics of Tethered Satellite Systems," AAS/AIAA Spaceflight Mechanics Meeting, Houston, TX, Feb. 1991 (AAS Paper 91-175).

[17]Fujii, H., Uchiyama, K., and Kokubun K., "Mission Function Control of Tethered Subsatellite Deployment/Retrieval: In-Plane and Out-of-Plane Motion," *Journal of Guidance, Control, and Dynamics*, Vol. 14, No. 2, 1991, pp. 471–473.

[18]Fujii, H., Kokubun K., and Uchiyama, K., "Control of Deployment/Retrieval of Subsatellite Connected by Flexible Tether," AIAA Paper 90-3324, Aug. 1990.

[19]Kim, E., and Vadali, S. R., "Effects of Longitudinal Vibrations on the Performance of Feedback Control Laws for the Tethered Satellite System," *Proceedings of the Eighth VPI-SU Symposium on Dynamics and Control of Large Space Structures*, Blacksburg, VA, 1991, pp. 667–678.

[20]He, X., and Powell, J. D., "Tether Damping in Space," *Journal of Guidance, Control, and Dynamics*, Vol. 13, No. 1, 1990, pp. 104–112.